DR. MARIANA ANDREA ROJAS (Orcid ID : 0000-0002-8712-0958)
DR. LORENZO MARINI (Orcid ID : 0000-0001-6662-2644)
PROF. CINZIA MARCHESE (Orcid ID : 0000-0002-9280-8917)

Article type : Original Article Clinical Periodontology

Dr. Mariana Andrea Rojas (Orcid: 0000-0002-8712-0958)
Prof. Simona Ceccarelli (Orcid: 0000-0001-8789-7719)
Dr. Giulia Gerini (Orcid: 0000-0002-9229-5103)
Dr. Enrica Vescarelli (Orcid: 0000-0003-3131-948X)
Dr. Lorenzo Marini (Orcid: 0000-0001-6662-2644)
Prof. Cinzia Marchese (Orcid: 0000-0002-9280-8917)
Prof. Andrea Pilloni (Orcid: 0000-0002-6268-1863)

Article type: Original Article Clinical Periodontology

i. TITLE:

Gene Expression Profiles Of Oral Soft Tissue Derived Fibroblasts From Healing Wounds: Correlation With Clinical Outcome, Autophagy Activation And Fibrotic Markers Expression.

ii. SHORT RUNNING TITLE:

Gene expression in oral wound healing

iii. Full names of the authors:

Mariana Andrea Rojas[1*], Simona Ceccarelli[2*], Giulia Gerini[2], Enrica Vescarelli[2], Lorenzo Marini[1], Cinzia Marchese[2], Andrea Pilloni[1]

[*] These authors contributed equally.

iv. Author's institutional affiliations:

[1] Section of Periodontics, Department of Oral and Maxillofacial Sciences, Sapienza, University of Rome, Rome, Italy.

[2] Department of Experimental Medicine, Sapienza University of Rome, Rome, Italy.

Conflict of interest and source of funding: the authors declare that they have no conflict of interests. The study was self-funded by the authors and their institution.

Corresponding author:

Mariana Andrea Rojas

Section of Periodontics,

Department of Oral and Maxillofacial Sciences,

Sapienza University of Rome,

6 Caserta Street, Rome 00161, Italy

Tel.: +39-0649-918152

Fax: +39-0644-230811

marianaandrea.rojas@uniroma1.it

Data Availability Statement:

The data that support the findings of this study are available from the corresponding author upon reasonable request.

v. Abstract and keywords

Abstract:

Aim: Our aim was to evaluate gene expression profiling of fibroblasts from human alveolar mucosa (M), buccal attached gingiva (G) and palatal (P) tissues during early wound healing, correlating it with clinical response.

Materials and Methods: M, G and P biopsies were harvested from six patients at baseline and 24 hrs after surgery. Clinical response was evaluated through Early Wound Healing Score (EHS). Fibrotic markers expression and autophagy were assessed on fibroblasts isolated from those tissues by Western blot and qRT-PCR. Fibroblasts from two patients were subjected to RT2 profiler array, followed by network analysis of the differentially expressed genes. The expression of key genes was validated with qRT-PCR on all patients.

Results: at 24 hrs after surgery, EHS was higher in P and G than in M. In line with our clinical results, no autophagy and myofibroblast differentiation were observed in G and P. We observed significant variations in mRNA expression of key genes: *RAC1*, *SERPINE1* and *TIMP1*, involved in scar formation; *CDH1*, *ITGA4* and *ITGB5*, contributing to myofibroblasts differentiation; *IL6* and *CXCL1*, involved in inflammation.

Conclusions: We identified some genes involved in periodontal soft tissues clinical outcome, providing novel insights into the molecular mechanisms of oral repair (ClinicalTrial.gov-NCT04202822).

Key words: gene expression profiling, gingiva, human biopsy, palate, wound healing.

vi. Clinical relevance:

Scientific rationale for the study: Clinical practice indicates differential healing between periodontal soft tissues, whereas literature provides scarce information comparing oral tissues repair in humans.

Principal findings: Clinical healing score was higher in the palate and gingiva with respect to oral mucosa. Accordingly, palate and gingiva showed lack of fibrotic markers and autophagy activation, explaining their scarless healing. Gene expression profiling in oral tissues demonstrated differential gene modulation after injury.

Practical implications: The discovery of key genes implicated in oral tissues differential healing can provide insights into the molecular mechanisms involved, allowing to develop new approaches of essential impact in periodontal surgery.

Introduction

Wound healing is a complex process orchestrated by a variety of known and unknown factors, divided into four stages (haemostasis, inflammation, proliferation and

remodelling) that occur in both skin and oral tissues (Hämmerle & Giannobile 2014). However, oral tissues present special features as rapid wound closure and reduced scar formation (Chen, Arbieva, Guo, Marucha & DiPietro, 2010; Iglesias-Bartolome et al., 2018; Simões et al., 2019; Szpaderska, Warburton et al., 2005; Zuckerman & DiPietro, 2003;).

In order to provide a better understanding of the complexity of the repair process, previous studies have examined the wound transcriptome through a microarray analysis comparing oral and dermal wound repair responses (Chen et al. 2010; Iglesias-Bartolome et al. 2018; Simões et al. 2019).

Chen et al., (2010) compared tongue wounds and dermal wounds gene expression at different healing time intervals in an animal model, and concluded that oral and skin wounds had a comparable degree of transcriptional changes, except for 12 and 24 hrs.

In a recent human study (Iglesias-Bartolome et al. 2018), epithelial tissues from oral and dermal wounds were analyzed, showing a keratinocyte-driven wound repair in healthy individuals and raising the possibility that the transcriptional regulatory networks responsible for the accelerated healing in oral mucosa are already present in the unwounded state.

Recently, Simões et al. (2019), evaluated differential microRNA profiles in dermal versus hard palate oral wounds on an animal model, showing an intrinsic genetic response that accelerates repair in oral tissues.

Nevertheless, the above mentioned studies used different oral wound models (cheek, tongue, buccal gingiva, palate) without taking into account their anatomical and functional differences. Moreover, two of them were performed in animals. However, while the biomolecular basis of the differences between oral and skin repair have been described, this is less understood regarding the different oral tissues.

To date, a global and comprehensive comparative profiling of the differently expressed genes in the human oral soft tissues after injury has not been reported. Nevertheless, a different clinical repair outcome between alveolar mucosa and attached

gingiva is a common finding, with a scar-free gingival repair (Larjava et al., 2011; Wong et al., 2009). In a previous human study (Vescarelli et al., 2017), we demonstrated an increase in αSMA expression and autophagy activation in alveolar mucosa 24 hrs after injury, but not in gingiva, resulting in a scarless outcome. Although a similar behavior could be expected in the palatal tissue (Chen et al., 2019; Simões et al., 2019), its peculiar characteristics (Squier & Finkelstein 2003) could account for a different outcome.

Fibroblasts are mesenchymal cells essential for wound healing and the repair processes, since they are responsible for the production of most of the extracellular matrix (ECM) in connective tissues. In latest years, the role of fibroblasts and myofibroblasts as key players in tissues repair has been extensively reported and it has become clear that fibroblasts from different tissues present several distinct features (Chiquet et al.,2015). In periodontal wound healing, the regeneration of connective tissues involves cellular activities driven by fibroblasts populations, such as secretion of matrix molecules and the organization of these matrix components into functionally active fibers that finally restore the periodontium (Chiquet et al.,2015; Smith et al., 2019).

A better understanding of the role of these cells in the wound healing of periodontal soft tissues, through a genetic profile analysis, could be of fundamental importance, in order to identify selected pathways and molecules that could open the way to the development of targeted approaches directed to the mesenchymal component of periodontal tissues, optimizing the wound microenvironment.

Therefore, the aim of the present study was to analyze and compare the gene expression profiling of fibroblasts from human alveolar mucosa (M), gingival (G) and palatal (P) tissues in the early phases following surgical wounding, correlating it with the clinical response, autophagy activation and fibrotic markers expression.

Materials and Methods

1. Ethics statements

The study protocol (ClinicalTrial.gov-NCT04202822) was approved by Sapienza University of Rome Ethics Committee (Ref.5315-Prot.2018/19). Each participant signed an informed consent in accordance with the Declaration of Helsinki (1975, revised in 2013).

2. Study design and patient selection

The present pilot study included six healthy adult patients (mean age 42.83±13.28, Table S1). Inclusion criteria were: (1) patients who underwent periodontal surgery to treat residual periodontal pockets at completion of non-surgical periodontal therapy; (2) patients with periodontal healthy status (Full-mouth Plaque Score and Full-Mouth Bleeding Score <15%, Lang & Bartold, 2018); (3) patients who agreed to be "volunteer" for biopsy collection procedures by signing an informed consent. Patients who underwent antibiotic or anti-inflammatory drugs consumption during the previous six months, patients in pregnancy or lactation period and smokers were excluded from the study.

Biopsies from alveolar mucosa (M), buccal attached gingiva (G) and palatal tissue (P) were harvested from vertical releasing incisions (VRIs) at baseline and 24 hrs after surgical procedures, replicating the wound model used in our previous study (Vescarelli et al., 2017). Clinical response was evaluated at 24 hrs and 1 week after surgery by means of the Early Wound Healing Score (EHS; Marini, Rojas, Sahrmann, Aghazada & Pilloni, 2018; Marini et al., 2019; Table S2).

Primary cultures of fibroblasts derived from biopsies of the three tissues were subjected to Western blot and qRT-PCR analyses to assess the expression of fibrotic markers and autophagy activation. Cells obtained from biopsies of two patients were processed for gene expression profiling and a network analysis of the differentially expressed genes (DEGs) was performed. The expression of the following key genes was then validated through qRT-PCR on cDNAs from cells obtained from the biopsies of each patient and on pooled cDNAs of all the enrolled patients: *ras-related C3 botulinum toxin substrate 1 (RAC1), serpin family E member 1 (SERPINE1), TIMP metallopeptidase inhibitor 1 (TIMP1), cadherin 1 (CDH1), integrin subunit alpha 4 (ITGA4), integrin subunit beta 5 (ITGB5), interleukin 6 (IL6) and C-X-C motif chemokine ligand 1 (CXCL1).*

The experimental design is presented in Figure 1.

3. Surgical procedures

All the surgical procedures and biopsies were performed by the same operator (MR). Following local anesthesia, M, G, and P baseline biopsies were harvested immediately prior to the surgical procedure at the level of the VRIs with a biopsy punch of 2.0 mm diameter. At the end of the surgical procedure primary closure was obtained with interrupted sutures. During this period, patients were instructed not to use mouth-rinses.

The final M, G and P biopsies were harvested at the level of VRIs 24 hrs after surgery. These areas healed by second intention and sutures were removed at 1 week.

4. Cell cultures

Primary cultures of human fibroblasts from M, G and P biopsies were established as previously described (Vescarelli et al., 2017). Briefly, the biopsy samples were cut into small pieces. All fragments were transferred into a centrifuge tube and subjected to enzymatic dissociation. Fragments were gently pipetted until disintegration into a single cell suspension. Cells were then seeded onto collagen IV (10 mg/ml)-coated culture plates and maintained in Dulbecco's Modified Eagle's Medium (DMEM; Sigma Aldrich, MI, Italy), supplemented with 10% fetal bovine serum (FBS; Sigma Aldrich) and antibiotics (Penicillin/Streptomycin). Experiments were performed at the same time for the three tissues, so M, G and P cells of each patient were analyzed at the same cell passage (3-8).

5. RT^2 Profiler PCR array

Total RNA of M, G and P cells from two patients was extracted using TRIzol reagent (Invitrogen, Carlsbad, CA, USA) following the manufacturer's instructions. RNA samples were quantified using a NanoDrop ND-1000 spectrophotometer (NanoDrop, Wilmington, DE, USA). cDNAs obtained were used for gene expression profiling using the Human Wound Healing RT^2 Profiler™ PCR Array (Qiagen, MI, Italy), according to the manufacturer's instructions. Fold changes in expression between baseline and 24 hrs or between the three tissues at baseline were determined with the $2^{-\Delta\Delta CT}$ method. Heatmap and Venn diagrams were generated using the web-based tools Morpheus (https://software.broadinstitute.org/morpheus/) and Venn (http://bioinformatics.psb.ugent.be/webtools/Venn/), respectively.

6. Clinical analysis

A blinded examiner evaluated the clinical wound healing response at the level of the VRIs in M, G and P tissue 24 hrs after surgery (before harvesting the biopsies) using the EHS. The same evaluation was performed 1 week after the surgical procedure, immediately before suture removal.

7. Bioinformatics analysis

Gene ontology (GO) analysis was performed using Protein Analysis Through Evolutionary Relationships (PANTHER) classification system software (http://www.pantherdb.org). The protein-protein interaction (PPI) network was constructed from STRING database (https://string-db.org/) then visualized and edited with Cytoscape software (version 3.8.0). The APP plug−ins Molecular Complex Detection (MCODE) and cytoHubba were used to cluster densely connected genes and to identify important hub genes of the entire network, respectively.

8. Quantitative real- time PCR (qRT-PCR)

qRT-PCR was performed on RNA from cell cultures of six patients, as previously described (Nodale et al., 2014a).

9. Western blot analysis

Cells were lysed in RIPA buffer and processed for Western blot analysis as previously described (Nodale et al., 2014b). Densitometric analysis was performed with Quantity One Program (Bio-Rad Laboratories S.r.l., Segrate, MI, Italy) as previously described (D'Amici et al., 2013).

10. Statistical analysis

Data were analysed on Prism 8.0 (GraphPad Software, La Jolla, USA) and are shown as mean ± SD from three independent experiments conducted in triplicate. Two-tailed unpaired Student's *t* test was used for statistical analysis. For continuous variables (EHS score), median and the interquartile range (IQR) were calculated, and the

nonparametric Mann-Whitney U test was used for statistical analysis. *P* values < .05 was considered statistically significant. DEGs were identified via fold change filtering using $p < .05$ and a cut-off of absolute fold change > 2.

Detailed materials and methods are provided in the Appendix.

Results

1. Clinical wound healing response

All the surgical procedures were uneventfully and successfully completed.

24 hrs post-surgery, the median EHS value in P (10, IQR 3) and in G (7, IQR 0.75) were significantly higher than in M (6, IQR 1.25). At this time, P showed the highest EHS value and the difference was significant with the G and M tissues. At 1 week, no significant differences were found between M and G tissues, while P values were still significantly higher than M (Figure 2, Table 1).

2. Myofibroblasts differentiation and autophagy activation in palatal wound healing

Fibroblast-like cells were isolated to analyze αSMA expression at both mRNA and protein level. qRT-PCR analysis in a pool of six patients confirmed αSMA increase in M (2.2-fold) and decrease in G (0.3-fold) at 24 hrs. P behaved like G, with a significant decrease in αSMA expression at 24 hrs (0.3-fold) (Figure 3A). The results of qRT-PCR analysis were highly consistent on an inter-individual basis: αSMA was upregulated in M at 24 hrs in all the six patients, while for G and P a decrease in αSMA at 24 hrs was observed in four and five out of six patients, respectively (Figure S1).

Such data were also confirmed at protein level, and the same trend was observed for the fibrotic marker Collagen 1a1 (Col1a1) (Figure 3B, C). Noteworthy, we also observed a differential expression of both αSMA and Col1a1 between the three tissues at baseline, with higher levels in G and P than in M (Figure S2).

We then analyzed the activation of AKT, a key mediator of cell survival and differentiation and a well-known inhibitor of autophagy (Lotti et al., 2007). We observed a reduction of AKT phosphorylation at 24 hrs in M (0.4-fold), with no significant variations in G and P (Figure 3D, E).

Autophagy was not active in G and P, since no modulation of LC3-II/LC3-I ratio and P62 expression between baseline and 24 hrs was observed. However, it was active in M, which displays increased LC3-II/LC3-I ratio (2.0-fold) and P62 degradation (0.6-fold) (Figure 3D, E).

3. Differentially expressed genes (DEGs) associated with early wound healing

Of the 84 examined genes, 52 showed a > 2-fold differential expression at 24 hrs *vs* baseline, in at least one of the three tissues in both patients (Table S3). In unwounded tissues (baseline), 39 of the total examined genes showed differential expression between at least two of the three tissues (Table S4).

Hierarchical heatmap showed that M and G samples of Patient 1 and 4 presented similar patterns, clustering together on the column side, while P samples varied between the two patients (Figure 4A).

Through the intersection of M, G and P datasets in Venn diagrams, we found the highest number of overlapping DEGs between M and P for the upregulated genes (Figure 4B), while in the downregulated datasets, this was observed between G and P (Figure 4C).

4. Gene enrichment analysis and PPI network

The Gene Ontology (GO) analysis of DEGs (Figure 4D), showed the most enriched biological process (BP, Table S5) cellular component (CC, Table S6) and molecular function (MF, Table S7) GO terms (FDR < 0.05).

A protein-protein interaction (PPI) network including 52 nodes and 258 edges was obtained by applying STRING data to Cytoscape software (Figure 4E). The enriched number of interactions among these DEGs is due to their biological connections as involved in wound healing. By using MCODE plug-in, we found two clusters with 21 nodes and 189 edges (score=18.9) for the first one and 8 nodes and 28 edges (score=8)

for the second (Figure 4F). Applying the cytoHubba plug-in, we detected 15 hub genes of the network using the MCC method (Figure 4G, Table S8).

Eight genes were subsequently selected: *RAC1, SERPINE1, TIMP1, CDH1, ITGA4, ITGB5, IL6* and *CXCL1*, based on their differential modulation between M, G and P in the two patients (Figure 4H), their inclusion in the most relevant clusters, their identification as hub genes and their potential role in wound repair (Basso et al., 2016; Buskermolen, Roffel & Gibbs, 2010; Jakhu, Gill & Singh, 2018; Kuwahara Hatoko, Tada & Tanaka, 2002; Romagnani, Lasagni, Annunziato, Serio & Romagnani, 2004; Simone & Higgins, 2015).

The fold expression of the selected genes in Patient 1 and Patient 4 is reported in Table 2. PCR array substantially showed a differential expression between M on one side, and G and P on the other. In M we observed down-regulation of *RAC1*, *SERPINE1*, *TIMP1*, *ITGB5*, and up-regulation of *IL6*. In G and P, *CDH1* resulted to be down-regulated, and *ITGA4* up-regulated. Some discordance between the two patients was observed, especially for *CXCL1* (Figure 4H).

5. qRT-PCR Validation

Significant alterations in mRNA expression at 24 hrs *vs* baseline in at least one of the three tissues were confirmed (Figure 5A).

RAC1 confirmed to be down-modulated at 24 hrs in M (0.5 -fold) and no significantly modulated in P, as in PCR array, while by qRT-PCR it resulted up-regulated in G (1.7-fold, Figure 5B).

As for *SERPINE1* and *TIMP1,* we observed a discrepancy between PCR array and qRT-PCR, since in the latest these two genes appeared to be up-modulated in M (1.8-fold and 2.6-fold, respectively) and down-modulated in P (0.7-fold and 0.2-fold respectively), with no significant changes in G (Figure 5C, D).

CDH1 confirmed to be decreased in G and P (0.1 and 0.2-fold, respectively), while the up-regulation in M detected in Patient 4 was not confirmed, since we observed no significant variations, as in Patient 1 (Figure 5E).

ITGA4 and *ITGB5* displayed an opposite behavior in P, with a significant increase for the first (2.5-fold) and a decrease for the latest (0.6-fold) (Figure 5F, G). This modulation was contrary to PCR array results, in which we observed variability between

the two patients. Regarding M and G, *ITGA4* resulted decreased (0.8-fold) and increased (1.2-fold), respectively, while no variations were observed for *ITGB5.*

qRT-PCR validation for IL6 showed discrepancy with PCR array, with no variations in M and down-modulation in G and P (0.7-fold) (Figure 5H). Finally, *CXCL1* confirmed the opposite modulation in G (0.3-fold decrease) and P (2.2-fold increase). An up-modulation (4.9-fold) revealed in M (Figure 5I) have been observed in PCR array only for Patient 1.

The significant variations observed by qRT-PCR on pooled cDNAs were highly consistent on an inter-individual basis: in particular, at 24 hrs *RAC1* was down-modulated in M and up-regulated in G in all the patients (Figure 6A, I); *SERPINE1* down-modulation in P was observed in all the patients, while M resulted to be up-regulated in four out of six patients (Figure 6B, J); *TIMP1* up-modulation in M was confirmed in five out of six patients, and down-modulation in P was found in all the six patients (Figure 6C, K); *CDH1* confirmed to be decreased in G and P in six and five patients, respectively (Figure 6D, L); *ITGA4* down-modulation in M was observed in all the patients, while increase in G and P was detected in five out of six patients (Figure 6E, M); as for *ITGB5*, the significant down-modulation in P was confirmed in all the patients (Figure 6F, N); *IL6* showed some inter-individual variations in M, while down-modulation in G and P was confirmed in six and five patients, respectively (Figure 6G, O); *CXCL1* showed up-modulation in M and P in four out of six patients, while down-modulation in G was confirmed in all the patients (Fig. 6H, P).

The differential expression of the genes of interest in unwounded M, G and P cells is reported in Figure S3, and details of the results at baseline are included in the Appendix.

Discussion

Oral wound healing presents an accelerated rate with respect to cutaneous wounds (Iglesias-Bartolome et al., 2018). However, wound healing response varies between the different oral sites, ranging from absence to extensive scar formation (Larjava et al., 2011).

Multiple cells types are involved in the wound repair process. Nevertheless, during wound healing, fibroblasts have a fundamental role, since they are primarily responsible for synthesis of the replacement ECM (Buskermolen, 2017; Sandulache et al., 2005; Smith et al., 2019).

Currently, the intrinsic characteristics that mediate healing at different oral soft tissues are poorly understood, mainly in humans.

In the present study, EHS, a score assessing clinical signs of re-epithelialization (CSR), haemostasis (CSH) and inflammation (CSI) (Marini, Rojas, Sahrmann, Aghazada & Pilloni, 2018; Marini et al., 2019), was used to evaluate the clinical healing response of M, G and P tissues 24 hrs and 1 week after injury.

We found higher mean EHS values in G and P with respect to M at 24 hrs. Noteworthy, the highest value was observed in P, raising the possibility of a better wound healing capacity of this tissue. However, at 1 week less significant differences were found, confirming the need to investigate the peculiar characteristics of oral repair preferentially at an early phase.

To our knowledge, this is the first human study investigating gene expression profiling of fibroblasts from three different oral soft tissues.

Using paired human M, G and P biopsies samples, we assessed myofibroblasts activation and autophagy. In accordance with our previous study (Vescarelli et al., 2017), we confirmed αSMA and Col1a1 increase and autophagic activation in M at 24 hrs and the opposite situation in G. Here, we demonstrate for the first time that in P cells the autophagic pathway is not active, and both αSMA and Col1a1 are downregulated 24 hrs after injury, suggesting that P behaves like G, with low expression of fibrotic markers. This is in line with the observation of reduced scar formation in this tissue and with our clinical evaluation (EHS).

The low αSMA expression found in P at 24 hrs is in line with the suppression of wound contraction, mainly mediated by myofibroblasts, in this tissue, due to the tight attachment of the connective tissue to the palatal bone. Since wound contraction induces substantial scarring (El Ayadi, Jay & Prasai, 2020), our findings are in line with the better clinical response observed in P, in which connective tissue remodelling via cellular

response might be more important than myofibroblast differentiation (Jinno, Takahashi, Tsuchida, Tanaka & Moriyama, 2009).

In the last years, gene profiling analysis has gained clinical importance aiming to develop new approaches for non-healing or impaired wounds treatment (Peake et al., 2014). Therefore, we performed a gene expression profiling of fibroblasts from oral soft tissues using the Wound Healing RT^2 Profiler PCR array, demonstrating differential gene modulation between M, G and P 24 hrs after injury.

Among the 84 genes examined, 52 showed a > 2-fold differential expression at 24 hrs *vs* baseline, in accordance with previous studies that reported the greatest cellular changes at 12-24 hrs post-injury (Chen, Arbieva, Guo, Marucha & DiPietro, 2010).

The biological roles of the DEGs were studied using GO enrichment analyses. It is known that cell migration is the basis of re-epithelialization, playing a primary role in angiogenesis (Torres, Castro, Reyes & Torres, 2018). Consistent with this notion, our GO analysis showed that most of the enriched biological processes were related to cell movement, cell migration, extracellular matrix (ECM) organization and angiogenesis. Functionally, most of the DEGs are linked to chemokines, cytokines, integrins, collagen, but also to the inflammatory response, suggesting that inflammatory cytokines influence the wound healing response of different oral tissues. In fact, a direct correlation between reduced inflammation and scarless healing was previously demonstrated (Mak et al., 2009).

The 52 DEGs identified were subjected to PPI analysis, selecting the top 2 modules and 15 hub genes. On the basis of bioinformatic analysis and of the above mentioned results indicating a different healing response between M on one side and G and P on the other, we selected some genes with differential modulation between M and G/P (*RAC1*, *TIMP1, CDH1* and *IL6*). As PCR array revealed some similarities between M and P, we evaluate some genes with differential regulation between G and P (*SERPINE1, ITGA4, ITGB5* and *CXCL1*) to investigate potential divergences between them.

Validation of the selected genes in a pool of six patients confirmed a differential regulation of *RAC1, TIMP1, SERPINE1* and *ITGB5* in P with respect to both M and G,

while *CDH1, IL6* and *ITGA4* expression was similar between G and P, and only *CXCL1* showed a similar regulation in M and P.

The role of these genes in wound healing has been investigated in previous studies.

Deletion or inhibition of *RAC1* -a member of the Rho family of small GTPases- causes delayed oral wound healing by impairing the re-epithelialization process (Liu, Kapoor & Leask, 2009; Castilho et al., 2010). Conversely, increased *RAC1* promotes healing of oral mucositis lesions (Han et al., 2013) and *RAC1*-based biologic products have been proposed for impaired cutaneous wound healing (Fan et al., 2018).

Consistent with these findings, our analysis showed *RAC1* down-modulation in M and up-regulation in G, with higher CSR values for G, confirming the correlation between increased *RAC1* expression and increase basal cells proliferation. The re-epithelialization regulatory mechanism could be different in G and P, since although P showed the highest CSR values, no *RAC1* modulation was observed.

Transforming growth factor beta 1 (TGFβ1) is involved in tissue fibrosis regulating collagen production (Schrementi, Ferreira, Zender & DiPietro, 2008). Autocrine TGFβ1 production in the wound microenvironment increases *SERPINE1* expression, which in turn promotes collagen deposition, favoring fibrosis and hypertrophic scars (Simone & Higgins, 2015). *TGFβ1* also promotes collagen deposition by inhibiting the matrix metalloproteinases (MMPs) that mediate collagen degradation and inducing *TIMP1* expression (Barrientos, Stojadinovic, Golinko, Brem & Tomic-Canic, 2008).

In our previous study (Vescarelli et al., 2017), we observed a persistent activation of myofibroblast induced by TGFβ1-stimulated autophagy, resulting in scar wound repair in M. In agreement with such findings, here we show up-regulation of both *SERPINE1* and *TIMP1* at 24 hrs in M. Interestingly, these two genes are down-modulated in P, in line with our clinical results showing the highest CSR and CSI values.

We believe that, together, *SERPINE1* and *TIMP1* might play a role in regulating scar formation in oral tissues. However, a recent human study reported *SERPINE1* up-modulation in P 5 days after excisional injury (Wang & Tatakis, 2017). This discrepancy could be due to differences in evaluation timing or in the wound repair model.

Noteworthy, no changes were observed for both *SERPINE1* and *TIMP1* in G. Such

results led us to hypothesize a differential myofibroblasts regulation between P and G, through *SERPINE1*-dependent and -independent pathways, respectively. In fact, when uninjured tissues were evaluated we observed that αSMA and Col1A1 expression are lower in M than P and G, in which baseline values are very high. This means that an up-regulation mechanism develops in oral mucosal tissues and a down-regulation mechanism in palatal and gingival tissues. We could even infer from our results a different mechanism between G and P, since αSMA expression at baseline is significantly higher in the former. This is in accordance with our results regarding *SERPINE1* gene expression, since P and G seems to have different down-regulation pathways to reach the same αSMA expression values observed at 24 hrs.

During wound healing, epithelial cells migrate to the wound area through epithelial-mesenchymal transition (EMT) process. Autophagy inhibition might induce EMT, revealed by down-regulation of the epithelial marker *E-cadherin (CDH1*) (Hill et al., 2019). Our results agree with this, since we observed *CDH1* reduction where autophagy is absent (G and P). Instead, *CDH1* did not change in M, where autophagy is active.

Integrins are critical components of the cell attachment machinery, promoting myofibroblasts differentiation and αSMA stress fibers assembly. *ITGB5* increase correlates with fibrosis in many tissues (Jakhu, Gill & Singh, 2018). Therefore, our findings of *ITGB5* down-modulation only in P are consistent with the observation of lower myofibroblasts activation in this tissue, resulting in a scarless healing. *ITGA4,* involved in cell attachment to the ECM and tissue remodelling (Jakhu, Gill & Singh, 2018), showed down-modulation in M, slight up-modulation in G and consistent overexpression in P. In this light, a proper *ITGA4* stimulation during early wound healing could be essential to ensure integrin-dependent migration and leukocytes recruitment, providing efficient tissue repair.

Since inflammation is a key determinant of fibrosis (Mak et al., 2009), we must consider the role of chemokines and cytokines as modulators of the initial inflammatory phase. *Interleukin 6 (IL6)* -one of the hub genes with the highest score in our network- promotes tissue regeneration and repair by indirectly favoring collagen production through induction of TGFβ1 gene expression (Basso et al., 2016). Therefore, *IL6* deficiency reduces collagen deposition and its attenuation leads to decrease of inflammatory cells recruitment and scar formation (Liechty, Adzick & Crombleholme,

2000). In our patients, we showed a significant reduction of *IL6* in both G and P. Such observation is consistent with the faster wound healing and reduced scarring observed in these tissues with respect to M.

Finally, we analyzed *CXCL1*, a pro-inflammatory chemokine that stimulates epithelial cell migration and promotes angiogenesis (Simone & Higgins, 2015), which significantly increased in M and in P, although to a lesser extent. Thus, our data suggest that the slight increase in P could account for a better re-epithelialization, as confirmed by higher values of CSR in this tissue than in G, in which *CXCL1* is down-modulated. Conversely, a more consistent increase, as that reported in M, might result in an excess of inflammatory signals, thus leading to scar formation.

The unwounded tissues gene expression evaluation in the present study showed relevant differences between the three tissues in both, DEGs and fibrotic markers expression, raising the possibility that the regulatory networks involved in the better oral wound repair capacity are already present, albeit partially, in the uninjured state. This is in agreement with previous studies (Chen et al. 2010; Iglesias-Bartolome et al. 2018; Simões et al. 2019).

Our research aimed at identifying the differential mechanism of early wound repair in fibroblasts derived from three oral soft tissues. We chose not to analyze total RNA isolated from the biopsies, although it could be more representative of the 'in-situ' situation, but to focus on the role of the mesenchymal component in wound healing, and especially of fibroblasts, the principal cell type present in the connective tissues (Sriram et al., 2015; Smith et al., 2019). Since their primary functions are to differentiate into myofibroblasts, to synthetize and maintain the ECM and to promote an inflammatory response (Kendall & Feghali-Bostwick, 2014; Häkkinen, Larjava & Fournier, 2014), fibroblasts can be considered to be key players in the wound healing process.

Moreover, in the latest years, translational research focused on oral fibroblasts, aiming to develop oral cell-based therapy that takes advantage of the potential regenerative properties of this cells to improve the wound healing of other tissues, such as the skin (Jiang & Rinkevich, 2020). Therefore, deepening into the knowledge of biomolecular mechanisms that regulate fibroblasts and myofibroblasts behavior in the

repair process is of interest for future wound healing and regenerative therapies. For this purpose, an analysis of the genetic profile was carried out in the present study through primary cultures of human fibroblast obtained from M, G and P biopsies.

It is known that many cell types alter their morphology and gene expression profile when grown on chemically equivalent surfaces with different rigidities (Yeung et al., 2005). In particular, culturing on stiff substrates and passaging might affect fibroblast phenotype *in vitro* (Landry, Rattan & Dixon, 2019). In this regard, it is important to clarify that in our previous study (Vescarelli et al., 2017) we have analyzed αSMA expression of cells derived by M and G at various passages (2 to 8), confirming no significant variability due to cell culture. In the present work, the experiments were performed at the same time for the three tissues in each patient. Some variability of passage number occurred between patients, since some patients required a further cell expansion to reach an adequate cell number for experimental setting. However, independent experiments (triplicate) were repeated also using cell at different passages, with reproducible results.

We demonstrated concordance between the results of the present work and our previous study, showing that P tissue behavior is similar to G when myofibroblasts differentiation and autophagic activation were evaluated. In a very recent study evaluating palatal wound healing with primary intention in a rat model, the authors demonstrated that αSMA was not influenced by surgical trauma at 7 days (Chaushu, Gavrielov, Chaushu & Vered, 2020). The results of this *in vivo* study are consistent with our observation of αSMA modulation at 24 hrs from the incision, thus contributing to support the hypothesis that main changes in the wound healing process occur in a very early stage.

However, we cannot exclude that αSMA expression in the three tissues could change in a later time period, since it has been also demonstrated that myofibroblasts differentiation (during tissue remodeling phase) may last for several days after wounding and this time is highly variable depending on several factors, including the wound size and whether the injury has healed by primary or secondary intention (Smith, Martínez, Martínez & McCulloch, 2019). So, we believe that it could be interesting -replicating this

experimental model-, to extend the evaluation period allowing a dynamic myofibroblasts differentiation evaluation.

Some discrepancies between the PCR array and qRT-PCR validation experiments results were observed in the present study. The potential impact of inter-individual variations of the selected genes on pooled qRT-PCR results was evaluated by performing qRT-PCR validation in each patient. The results obtained indicated a good consistency between patients; indeed, the significant up-regulation or down-modulation of the eight genes at 24 hrs assessed in the pooled cDNAs were observed in the majority of patients, thus confirming the trend of each gene in the three tissues. In particular, qRT-PCR validation on Patient 1 and Patient 4 confirmed the discrepancies with PCR array, demonstrating that they are not due to inter-individual variations. The differential expression of some genes between PCR array and qRT-PCR could be explained by technical differences in probe locations, by cross-hybridization of the probes on the array with other targets, or simply by variations in normalization, since PCR array use five different housekeeping genes while qRT-PCR expression is normalized only with respect to GAPDH.

This is the first study comparing gene expression profiles of fibroblasts derived from three different oral soft tissues in the healing process. Nevertheless, some limitations of our study should be addressed. The RT2 profiler array was performed in fibroblasts derived from the tissues of only two patients and this could generate a variation in the results. Furthermore, the tissue evaluation was limited to one cell type, and future studies assessing genetic profiles of whole periodontal tissues are encouraged.

In conclusion, in the present study we focused on specific genes involved in the early wound healing process, showing different regulation pattern between the three periodontal soft tissues, which could account for their differential clinical outcome after surgery. A deeper gene analysis will require further studies to confirm these results, potentially including more patients, which was not possible here due to the strict enrolment conditions. Nonetheless, we think that our findings may contribute to elucidate

the mechanisms behind the differential clinical repair outcomes of alveolar mucosa, buccal attached gingiva and palatal tissue, providing the basis for further investigations focused on deepening the knowledge about specific molecular pathways correlated with the most relevant DEGs here reported.

References

Barrientos, S., Stojadinovic, O., Golinko, M. S., Brem, H., & Tomic-Canic, M. (2008). Growth factors and cytokines in wound healing. *Wound repair and regeneration: official publication of the Wound Healing Society [and] the European Tissue Repair Society*, *16*(5), 585–601. https://doi.org/10.1111/j.1524-475X.2008.00410.x

Basso, F. G., Pansani, T. N., Turrioni, A. P., Soares, D. G., de Souza Costa, C. A., & Hebling, J. (2016). Tumor Necrosis Factor-α and Interleukin (IL)-1β, IL-6, and IL-8 Impair In Vitro Migration and Induce Apoptosis of Gingival Fibroblasts and Epithelial Cells, Delaying Wound Healing. *Journal of Periodontology*, *87*(8), 990–996. https://doi.org/10.1902/jop.2016.150713

Buskermolen, J. K., Roffel, S., & Gibbs, S. (2017). Stimulation of oral fibroblast chemokine receptors identifies CCR3 and CCR4 as potential wound healing targets. *Journal of Cellular Physiology*, *232*(11), 2996–3005. https://doi.org/10.1002/jcp.25946

Castilho, R. M., Squarize, C. H., Leelahavanichkul, K., Zheng, Y., Bugge, T., & Gutkind, J. S. (2010). Rac1 is required for epithelial stem cell function during dermal and oral mucosal wound healing but not for tissue homeostasis in mice. *PloS One*, *5*(5), e10503. https://doi.org/10.1371/journal.pone.0010503

Chaushu, L., Rahmanov Gavrielov, M., Chaushu, G., & Vered, M. (2020). Palatal Wound Healing with Primary Intention in a Rat Model-Histology and Immunohistomorphometry. *Medicina (Kaunas, Lithuania)*, *56*(4), 200. https://doi.org/10.3390/medicina56040200

Chen, L., Arbieva, Z. H., Guo, S., Marucha, P. T., Mustoe, T. A., & DiPietro, L. A. (2010). Positional differences in the wound transcriptome of skin and oral mucosa. *BMC Genomics*, *11*, 471. https://doi.org/10.1186/1471-2164-11-471

Chen, L., Simões, A., Chen, Z., Zhao, Y., Wu, X., Dai, Y., DiPietro, L. A., & Zhou, X. (2019). Overexpression of the Oral Mucosa-Specific microRNA-31 Promotes Skin Wound

Closure. *International Journal of Molecular Sciences*, *20*(15), 3679. https://doi.org/10.3390/ijms20153679

Chiquet, M., Katsaros, C., & Kletsas, D. (2015). Multiple functions of gingival and mucoperiosteal fibroblasts in oral wound healing and repair. *Periodontology 2000*, *68*(1), 21–40. https://doi.org/10.1111/prd.12076

D'Amici, S., Ceccarelli, S., Vescarelli, E., Romano, F., Frati, L., Marchese, C., & Angeloni, A. (2013). TNFα modulates Fibroblast Growth Factor Receptor 2 gene expression through the pRB/E2F1 pathway: identification of a non-canonical E2F binding motif. *PloSOone*, *8*(4), e61491. https://doi.org/10.1371/journal.pone.0061491

El Ayadi, A., Jay, J. W., & Prasai, A. (2020). Current Approaches Targeting the Wound Healing Phases to Attenuate Fibrosis and Scarring. *International Journal of Molecular Sciences*, *21*(3), 1105. https://doi.org/10.3390/ijms21031105

Fan, B., Wang, T., Bian, L., Jian, Z., Wang, D. D., Li, F., Wu, F., Bai, T., Zhang, G., Muller, N., Holwerda, B., Han, G., & Wang, X. J. (2018). Topical Application of Tat-Rac1 Promotes Cutaneous Wound Healing in Normal and Diabetic Mice. *International Journal of Biological Sciences*, *14*(10), 1163–1174. https://doi.org/10.7150/ijbs.25920

Hämmerle, C. H., & Giannobile, W. (2014). Working Group 1 of the European Workshop on Periodontology. Biology of soft tissue wound healing and regeneration–consensus report of Group 1 of the 10th European Workshop on Periodontology. *Journal of Clinical Periodontology,* 41(Suppl. 15), S1–S5.

Han, G., Bian, L., Li, F., Cotrim, A., Wang, D., Lu, J., Deng, Y., Bird, G., Sowers, A., Mitchell, J. B., Gutkind, J. S., Zhao, R., Raben, D., ten Dijke, P., Refaeli, Y., Zhang, Q., & Wang, X. J. (2013). Preventive and therapeutic effects of Smad7 on radiation-induced oral mucositis. *Nature Medicine*, *19*(4), 421–428. https://doi.org/10.1038/nm.3118

Hill, C., Li, J., Liu, D., Conforti, F., Brereton, C. J., Yao, L., Zhou, Y., Alzetani, A., Chee, S. J., Marshall, B. G., Fletcher, S. V., Hancock, D., Ottensmeier, C. H., Steele, A. J., Downward, J., Richeldi, L., Lu, X., Davies, D. E., Jones, M. G., & Wang, Y. (2019). Autophagy inhibition-mediated epithelial-mesenchymal transition augments local myofibroblast differentiation in pulmonary fibrosis. *Cell Death & Disease*, *10*(8), 591. https://doi.org/10.1038/s41419-019-1820-x

Iglesias-Bartolome, R., Uchiyama, A., Molinolo, A. A., Abusleme, L., Brooks, S. R., Callejas-Valera, J. L., Edwards, D., Doci, C., Asselin-Labat, M. L., Onaitis, M. W., Moutsopoulos, N. M., Gutkind, J. S., & Morasso, M. I. (2018). Transcriptional signature primes human oral mucosa for rapid wound healing. *Science Translational Medicine*, *10*(451), eaap8798. https://doi.org/10.1126/scitranslmed.aap8798

Jakhu, H., Gill, G., & Singh, A. (2018). Role of integrins in wound repair and its periodontal implications. *Journal of Oral Biology and Craniofacial Research*, *8*(2), 122–125. https://doi.org/10.1016/j.jobcr.2018.01.002

Jiang, D., & Rinkevich, Y. (2020). Scars or Regeneration? - Dermal Fibroblasts as Drivers of Diverse Skin Wound Responses. *International journal of molecular sciences*, *21*(2), 617. https://doi.org/10.3390/ijms21020617

Jinno, K., Takahashi, T., Tsuchida, K., Tanaka, E., & Moriyama, K. (2009). Acceleration of palatal wound healing in Smad3-deficient mice. *Journal of Dental Research*, *88*(8), 757–761. https://doi.org/10.1177/0022034509341798

Kendall, R. T., & Feghali-Bostwick, C. A. (2014). Fibroblasts in fibrosis: novel roles and mediators. *Frontiers in pharmacology*, *5*, 123. https://doi.org/10.3389/fphar.2014.00123

Häkkinen, L., Larjava, H., & Fournier, B. P. (2014). Distinct phenotype and therapeutic potential of gingival fibroblasts. *Cytotherapy*, *16*(9), 1171–1186. https://doi.org/10.1016/j.jcyt.2014.04.004

Kuwahara, M., Hatoko, M., Tada, H., & Tanaka, A. (2001). E-cadherin expression in wound healing of mouse skin. *Journal of Cutaneous Pathology*, *28*(4), 191–199. https://doi.org/10.1034/j.1600-0560.2001.028004191.x

Landry, N. M., Rattan, S. G., & Dixon, I. (2019). An Improved Method of Maintaining Primary Murine Cardiac Fibroblasts in Two-Dimensional Cell Culture. *Scientific reports*, *9*(1), 12889. https://doi.org/10.1038/s41598-019-49285-9

Lang, N. P., & Bartold, P. M. (2018). Periodontal health. *Journal of Clinical Periodontology*, *45 Suppl 20*, S9–S16. https://doi.org/10.1111/jcpe.12936

Larjava, H., Wiebe, C., Gallant-Behm, C., Hart, D. A., Heino, J., & Häkkinen, L. (2011). Exploring scarless healing of oral soft tissues. *Journal (Canadian Dental Association)*, *77*, b18.

Liechty, K. W., Adzick, N. S., & Crombleholme, T. M. (2000). Diminished interleukin 6 (IL-6) production during scarless human fetal wound repair. *Cytokine*, *12*(6), 671–676. https://doi.org/10.1006/cyto.1999.0598

Liu, S., Kapoor, M., & Leask, A. (2009). Rac1 expression by fibroblasts is required for tissue repair in vivo. *The American Journal of Pathology*, *174*(5), 1847–1856. https://doi.org/10.2353/ajpath.2009.080779

Lotti, L. V., Rotolo, S., Francescangeli, F., Frati, L., Torrisi, M. R., & Marchese, C. (2007). AKT and MAPK signaling in KGF-treated and UVB-exposed human epidermal cells. Journal of Cellular Physiology, 212(3), 633-642. doi: 10.1002/jcp.21056.

Mak, K., Manji, A., Gallant-Behm, C., Wiebe, C., Hart, D. A., Larjava, H., & Häkkinen, L. (2009). Scarless healing of oral mucosa is characterized by faster resolution of inflammation and control of myofibroblast action compared to skin wounds in the red Duroc pig model. *Journal of Dermatological Science,* 5, 168–180. https://doi.org/10.1016/j.jdermsci.2009.09.005

Marini, L., Rojas, M. A., Sahrmann, P., Aghazada, R., & Pilloni, A. (2018). Early Wound Healing Score: a system to evaluate the early healing of periodontal soft tissue wounds. *Journal of Periodontal & Implant Science*, *48*(5), 274–283. https://doi.org/10.5051/jpis.2018.48.5.274

Marini, L., Sahrmann, P., Rojas, M. A., Cavalcanti, C., Pompa, G., Papi, P., & Pilloni, A. (2019). Early Wound Healing Score (EHS): An Intra- and Inter-Examiner Reliability Study. *Dentistry Journal*, *7*(3), 86. https://doi.org/10.3390/dj7030086

Nodale, C., Ceccarelli, S., Giuliano, M., Cammarota, M., D'Amici, S., Vescarelli, E., Maffucci, D., Bellati, F., Panici, P. B., Romano, F., Angeloni, A., & Marchese, C. (2014a). Gene expression profile of patients with Mayer-Rokitansky-Küster-Hauser syndrome: new insights into the potential role of developmental pathways. *PloS One*, *9*(3), e91010. https://doi.org/10.1371/journal.pone.0091010

Nodale, C., Vescarelli, E., D'Amici, S., Maffucci, D., Ceccarelli, S., Monti, M., Benedetti Panici, P., Romano, F., Angeloni, A., & Marchese, C. (2014b). Characterization of human vaginal mucosa cells for autologous in vitro cultured vaginal tissue transplantation in patients with MRKH syndrome. *BioMed Research International*, *2014*, 201518. https://doi.org/10.1155/2014/201518

Peake, M. A., Caley, M., Giles, P. J., Wall, I., Enoch, S., Davies, L. C., Kipling, D., Thomas, D. W., & Stephens, P. (2014). Identification of a transcriptional signature for the wound healing continuum. *Wound repair and regeneration: official publication of the Wound Healing Society [and] the European Tissue Repair Society*, *22*(3), 399–405. https://doi.org/10.1111/wrr.12170

Polimeni, G., Xiropaidis, A. V., & Wikesjö, U. M. (2006). Biology and principles of periodontal wound healing/regeneration. *Periodontology 2000*, *41*, 30–47. https://doi.org/10.1111/j.1600-0757.2006.00157.x

Romagnani, P., Lasagni, L., Annunziato, F., Serio, M., & Romagnani, S. (2004). CXC chemokines: the regulatory link between inflammation and angiogenesis. *Trends in Immunology*, *25*(4), 201–209. https://doi.org/10.1016/j.it.2004.02.006

Sandulache, V. C., Dohar, J. E., & Hebda, P. A. (2005). Adult-fetal fibroblast interactions: effects on cell migration and implications for cell transplantation. *Cell transplantation*, *14*(5), 331–337. https://doi.org/10.3727/000000005783983025

Schrementi, M. E., Ferreira, A. M., Zender, C., & DiPietro, L. A. (2008). Site-specific production of TGF-beta in oral mucosal and cutaneous wounds. *Wound Repair and Regeneration: official publication of the Wound Healing Society [and] the European Tissue Repair Society*, *16*(1), 80–86. https://doi.org/10.1111/j.1524-475X.2007.00320.x

Simões, A., Chen, L., Chen, Z., Zhao, Y., Gao, S., Marucha, P. T., Dai, Y., DiPietro, L. A., & Zhou, X. (2019). Differential microRNA profile underlies the divergent healing responses in skin and oral mucosal wounds. *Scientific Reports*, *9*(1), 7160. https://doi.org/10.1038/s41598-019-43682-w

Simone, T., & Higgins, P. (2015). Inhibition of SERPINE1 Function Attenuates Wound Closure in Response to Tissue Injury: A Role for PAI-1 in Re-Epithelialization and Granulation Tissue Formation. *Journal of Developmental Biology*, *3*(1), 11–24. http://dx.doi.org/10.3390/jdb3010011

Smith, P. C., Martínez, C., Martínez, J., & McCulloch, C. A. (2019). Role of Fibroblast Populations in Periodontal Wound Healing and Tissue Remodeling. *Frontiers in physiology*, *10*, 270. https://doi.org/10.3389/fphys.2019.00270

Squier, C.A., Finkelstein, M.W. (2003). Oral mucosa. In A. Nanci (ed.), *Ten Cate's Oral Histology*. Mosby, St. Luois, MO.

Sriram, G., Bigliardi, P. L., & Bigliardi-Qi, M. (2015). Fibroblast heterogeneity and its implications for engineering organotypic skin models in vitro. *European journal of cell biology*, *94*(11), 483–512. https://doi.org/10.1016/j.ejcb.2015.08.001

Szpaderska, A. M., Zuckerman, J. D., & DiPietro, L. A. (2003). Differential injury responses in oral mucosal and cutaneous wounds. *Journal of Dental Research*, *82*(8), 621–626. https://doi.org/10.1177/154405910308200810

Torres, P., Castro, M., Reyes, M., & Torres, V. A. (2018). Histatins, wound healing, and cell migration. *Oral Diseases*, *24*(7), 1150–1160. https://doi.org/10.1111/odi.12816

Ueno, C., Hunt, T. K., & Hopf, H. W. (2006). Using physiology to improve surgical wound outcomes. *Plastic and Reconstructive Surgery*, *117*(7 Suppl), 59S–71S. https://doi.org/10.1097/01.prs.0000225438.86758.21

Vescarelli, E., Pilloni, A., Dominici, F., Pontecorvi, P., Angeloni, A., Polimeni, A., Ceccarelli, S., & Marchese, C. (2017). Autophagy activation is required for myofibroblast differentiation during healing of oral mucosa. *Journal of Clinical Periodontology*, *44*(10), 1039–1050. https://doi.org/10.1111/jcpe.12767

Wang, Y., & Tatakis, D. N. (2017). Human gingiva transcriptome during wound healing. *Journal of Clinical Periodontology*, *44*(4), 394–402. https://doi.org/10.1111/jcpe.12669

Warburton, G., Nares, S., Angelov, N., Brahim, J. S., Dionne, R. A., & Wahl, S. M. (2005). Transcriptional events in a clinical model of oral mucosal tissue injury and repair. *Wound Repair and Regeneration: official publication of the Wound Healing Society [and] the European Tissue Repair Society*, *13*(1), 19–26. https://doi.org/10.1111/j.1067-1927.2005.130104.x

Wikesjö, U. M., & Selvig, K. A. (1999). Periodontal wound healing and regeneration. *Periodontology 2000*, *19*, 21–39. https://doi.org/10.1111/j.1600-0757.1999.tb00145.x

Wong, J. W., Gallant-Behm, C., Wiebe, C., Mak, K., Hart, D. A., Larjava, H., & Häkkinen, L. (2009). Wound healing in oral mucosa results in reduced scar formation as compared

with skin: evidence from the red Duroc pig model and humans. *Wound Repair and Regeneration: official publication of the Wound Healing Society [and] the European Tissue Repair Society*, *17*(5), 717–729. https://doi.org/10.1111/j.1524-475X.2009.00531.x

Yeung, T., Georges, P. C., Flanagan, L. A., Marg, B., Ortiz, M., Funaki, M., Zahir, N., Ming, W., Weaver, V., & Janmey, P. A. (2005). Effects of substrate stiffness on cell morphology, cytoskeletal structure, and adhesion. *Cell motility and the cytoskeleton*, *60*(1), 24–34. https://doi.org/10.1002/cm.20041

Author contributions

M.A. Rojas, S. Ceccarelli contributed to conception, design, data acquisition, analysis and interpretation, drafted and critically revised the manuscript; G. Gerini, contributed to data acquisition and analysis and critically revised the manuscript; E. Vescarelli, contributed to data acquisition and critically revised the manuscript; L. Marini, contributed to design and critically revised the manuscript; C. Marchese, contributed to data acquisition and critically revised the manuscript; A. Pilloni contributed to conception, design, data analysis and interpretation and critically revised the manuscript.

All authors gave their final approval and agree to be accountable for all aspects of the work.

Table 1. Clinical wound healing response 24 hrs and 1 week after injury.

Patient	EHS					
	24 hrs			1 week		
	M	G	P	M	G	P
1	5 (R3,HO,I2)	6 (R3,H1,I2)	10 (R6,H2,I2)	9 (R6,H2,I1)	9 (R6,H2,I1)	10 (R6,H2,I2)
2	6 (R3,H2,I1)	7 (R3,H2,I2)	10 (R6,H2,I2)	9 (R6,H2,I1)	9 (R6,H2,I1)	10 (R6,H2,I2)
3	7 (R3,H2,I2)	9 (R6,H2,I1)	10 (R6,H2,I2)	9 (R6,H2,I1)	10 (R6,H2,I2)	10 (R6,H2,I2)
4	6 (R3,H2,I1)	7 (R3,H2,I2)	10 (R6,H2,I2)	9 (R6,H2,I1)	10 (R6,H2,I2)	10 (R6,H2,I2)
5	6 (R3,H2,I1)	7 (R3,H2,I2)	7 (R3,H2,I2)	6 (R3,H2,I1)	7 (R3,H2,I2)	10 (R6,H2,I2)
6	5 (R3,HO,I2)	7 (R3,H2,I2)	7 (R3,H2,I2)	7 (R3,H2,I2)	7 (R3,H2,I2)	10 (R6,H2,I2)
Median (IQR)	6 (1.25)	7 (0.75)	10 (3)	9 (2.25)	9 (3)	10 (0)

EHS, Early Wound Healing Score; M, alveolar mucosa; G, buccal attached gingiva; P, palate; R, clinical signs of re-epithelialization; H, clinical signs of haemostasis; I, clinical signs of inflammation; IQR, interquartile range.

Table 2: Differential expression of selected wound healing mediators in alveolar mucosal (M), buccal attached gingival (G) and palatal (P) cells derived from Patient 1 and Patient 4 between baseline and 24 hrs, identified by RT² Profiler PCR Array system.

Gene Symbol	*Gene Name*	Patient	Fold expression difference (24 hrs *vs* baseline)†					
			M		G		P	
			Up	Down	Up	Down	Up	Down
RAC1	*ras-related C3 botulinum toxin substrate 1 (rho family, small GTP binding protein Rac1)*	**1**	-	2.7	-	-	-	-
		4	-	2.0	-	-	-	-
SERPINE1	*serpin family E member 1*	**1**		5.3	-	-	-	-
		4	-	4.1	-	4.1	-	-
TIMP1	*TIMP metallopeptidase inhibitor 1*	**1**	-	5.1	-	-	-	-
		4	-	2.3	-	-	-	-
CDH1	*cadherin 1*	**1**	-	-	-	3.0	-	4.0
		4	2.2	-	-	4.0	-	2.6
ITGA4	*integrin subunit alpha 4*	**1**	-	-	2.7	-	-	2.2
		4	-	-	4.1	-	3.0	-
ITGB5	*integrin subunit beta 5*	**1**	-	2.6	-	-	2.0	-
		4	-	2.1	-	-	-	-
IL6	*interleukin 6*	**1**	3.1	-	-	-	-	-

		4	4.1	-	-	-	-	-
CXCL1	*C-X-C motif chemokine ligand 1*	**1**	48.9	-	-	23.8	-	-
		4	-	16.3	-	32.0	429.0	-

M, alveolar mucosa; G, buccal attached gingiva; P, palate. †Minimum cut-off expression difference was considered > 2-folds.

Figure legends

Figure 1. Experimental design. (A) Alveolar mucosa (M), buccal attached gingival (G) and palatal (P) biopsies were harvested at baseline and 24 hrs after surgery from six patients. **(B)** Clinical evaluation was performed at 24 hrs and 1 week after surgery by means of Early Healing Score (EHS). **(C)** *In vitro* experiments were performed on primary cultures of human fibroblasts derived from M, G and P tissue established at baseline and 24 hrs. In a pool of six patients, quantitative real-time PCR analysis of αSMA expression was performed to evaluate the extent of myofibroblast differentiation. Autophagic activation was evaluated through Western blot analysis. **(D)** Total RNA was extracted from primary cultures of human fibroblasts derived from M, G and P tissues biopsies. Gene expression profiling of wound healing genes was performed in M, G and P cells obtained from two different patients, using the Human Wound Healing RT² Profiler™ PCR Array. Then, the expression of eight selected genes (*RAC1, SERPINE1, TIMP1, CDH1, ITGA4, ITGB5, IL6* and *CXCL1*) was validated by means of qRT-PCR analysis on total RNA from M, G an P cells pooled from six patients, as well as from each patient separately.

Figure 2. Differential wound healing response after vertical releasing incision (VRI) in M, G and P. Clinical wound healing response was evaluated through assessment of Early Wound Healing Score (EHS) at 24 hrs and 1 week after surgery in M, G and P tissues. The median values of EHS were reported. Error bars represent interquartile range (IQR). *$p < .05$ *vs* 24 hrs; $^{\#}p < .05$ and $^{\#\#}p < .005$ *vs* M; $^{\dagger}p < .05$ *vs* G.

Figure 3. Fibrotic markers expression and autophagy pathway activation in M, G and P cells at baseline and 24 hrs after vertical releasing incision. (**A**) Quantitative real-time PCR analysis of αSMA mRNA expression in a pool of six patients. Relative mRNA levels are shown as fold value of the levels at baseline. mRNA levels were normalized to GAPDH mRNA expression. Each experiment was performed in triplicate. Error bars represent standard deviations. ***p* < .005 and ****p* < .0005 *vs* baseline. **(B)** Western blot analysis of αSMA and Collagen 1a1 (Col1A1) protein expression. β-Actin served as loading control. The images are representative of at least two independent experiments for each patient. **(C)** The intensity of the bands in (B) was evaluated by densitometric analysis, normalized and reported as relative expression with respect to baseline. **p* < .05 and ***p* < .005 *vs* baseline. **(D)** Western blot analysis of p-AKT, LC3 and P62 in M, G and P cells at baseline and 24 hrs. β-Actin was used as loading control. The images are representative of at least two independent experiments for each patient. **(E)** Densitometric analysis of p-AKT/β-Actin, LC3-II/LC3-I and P62/β-Actin was reported as relative expression with respect to baseline. Error bars represent standard deviations. **p* < .05 and ***p* < .005 *vs* baseline.

Figure 4. RT^2 Profiler PCR array to detect the expression of genes associated with wound healing and fibrosis in M, G and P cells. (A) Hierarchical clustering of 52 differentially expressed genes (DEGs) with a > 2-fold modulation in M, G and P cells of Patient 1 (green) and Patient 4 (orange). Blue and red indicate under- and over-expression at 24 hrs *vs* baseline. **(B, C)** Venn diagrams of the total number of up-regulated (B) or down-regulated (C) transcripts identified as statistically significant in the three sample groups (M, blue; G, pink; P, green) at 24 hrs *vs* baseline. Overlapping genes among the sample groups are represented in the areas of intersection between the three circles. **(D)** Gene Ontology (GO) analysis for biological process (BP), cellular components (CC) and molecular function (MF) obtained by PANTHER software. A false discovery rate (FDR) < 0.05 was settled as a threshold. Significantly overrepresented GO categories were visualized in the bar chart reporting the fold enrichment. **(E)** PPI network of DEGs, constructed using Cytoscape software. Nodes and font size are positively related to connectivity degree, which is further underlined by color gradient. Edges color

gradient is associated with STRING combined score, computed by combining the probabilities from the different evidence channels and corrected for the probability of randomly observing an interaction. **(F)** The two most relevant clusters visualized by MCODE in Cytoscape. Filters were based on the default parameters (Degree Cutoff =2; Node Score Cutoff =0.2; K-Core =2; Max.Depth =100). Nodes and font size are positively related to MCODE score, which is further underlined by color gradient. **(G)** Hub genes screened through the maximal clique centrality (MCC) algorithm from cytoHubba. Color gradient is positively related to MCC score. **(H)** Schematic representation of the differential expression of the eight selected genes in M, G and P cells of Patient 1 (P1) and Patient 4 (P4) at 24 hrs *vs* baseline by PCR array. ↓ blue squares indicate down-regulated genes; ↑ red squares indicate up-regulated genes.

Figure 5. Validation of differential gene expression by qRT-PCR in M, G and P cells. **(A)** Schematic representation of the differential expression of the eight selected genes in M, G and P cells at 24 hrs *vs* baseline by qRT-PCR. ↓ blue squares indicate down-regulated genes; ↑ red squares indicate up-regulated genes. **(B-I)** Quantitative real-time PCR analysis of mRNA expression levels of *RAC1* (B), *SERPINE1* (C), *TIMP1* (D), *CDH1* (E), *ITGA4* (F), *ITGB5* (G), *IL6* (H) and *CXCL1* (I) in a pool of six patients. For each gene, relative mRNA levels are shown as fold value of the levels at baseline. mRNA levels were normalized to GAPDH mRNA expression. Each experiment was performed in triplicate. Error bars represent standard deviations. *$p < .05$, **$p < .005$ and ***$p < .0005$ *vs* baseline.

Figure 6. Inter-individual gene expression by qRT-PCR in M, G and P cells. (A-H) Quantitative real-time PCR analysis of mRNA expression levels of *RAC1* (A), *SERPINE1* (B), *TIMP1* (C), *CDH1* (D), *ITGA4* (E), *ITGB5* (F), *IL6* (G) and *CXCL1* (H) in M, G and P cells obtained from each of the six patients separately (P1-P6). Relative mRNA levels are shown as fold value of the levels at baseline. mRNA levels were normalized to GAPDH mRNA expression. Each experiment was performed in triplicate. Error bars represent standard deviations. *p < .05, **p < .005 and ***p < .0005 *vs* baseline. (I-P) Ratio of *RAC1* (I), *SERPINE1* (J), *TIMP1* (K), *CDH1* (L), *ITGA4* (M), *ITGB5* (N), *IL6* (O) and *CXCL1* (P) expression at 24 hrs/Baseline in M, G and P cells obtained from each of the

six patients (P1-P6), expressed in logarithmic scale, where values >1 represent gene expression increase at 24 hrs and values <1 represent decrease. Error bars represent standard deviations. *p < .05, **p < .005 and ***p < .0005 *vs* baseline.

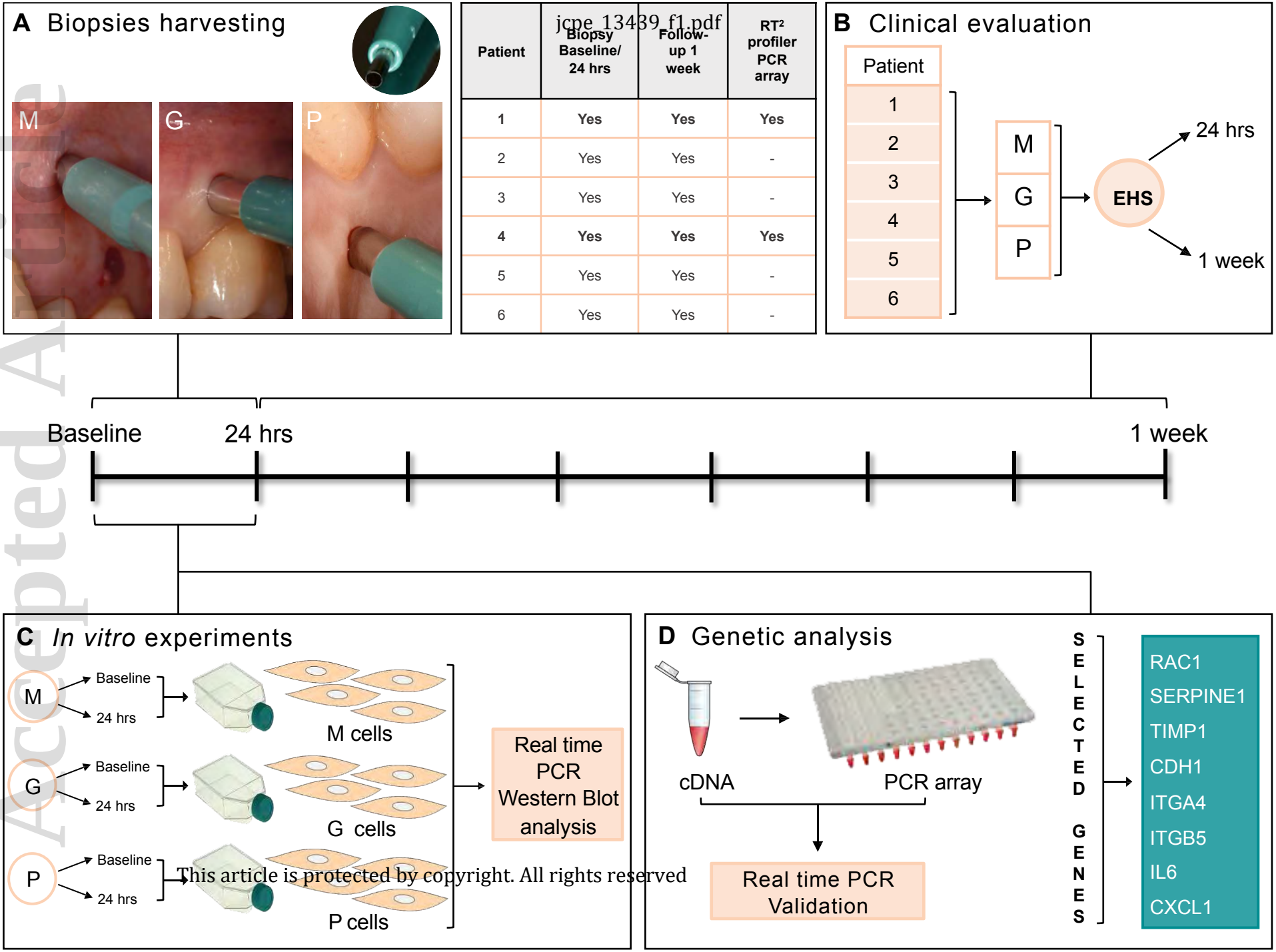

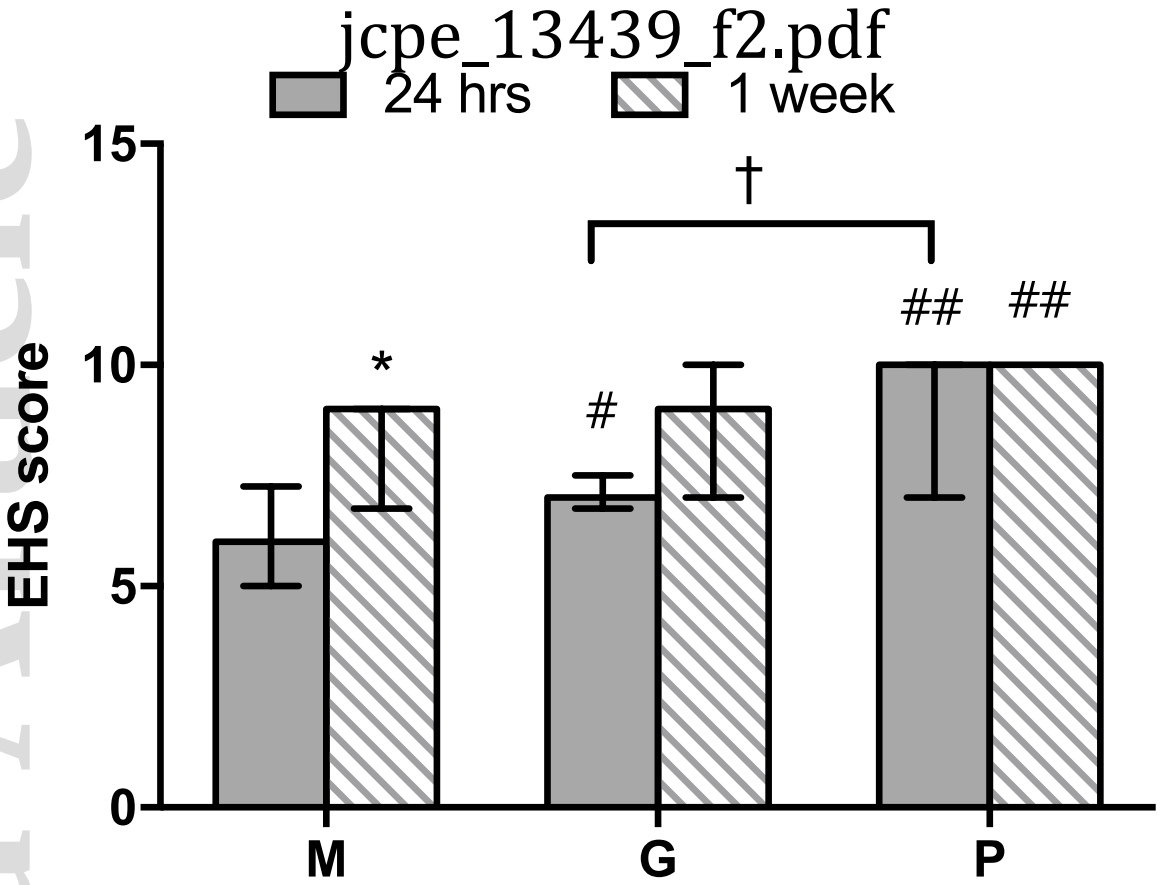

Figure 2

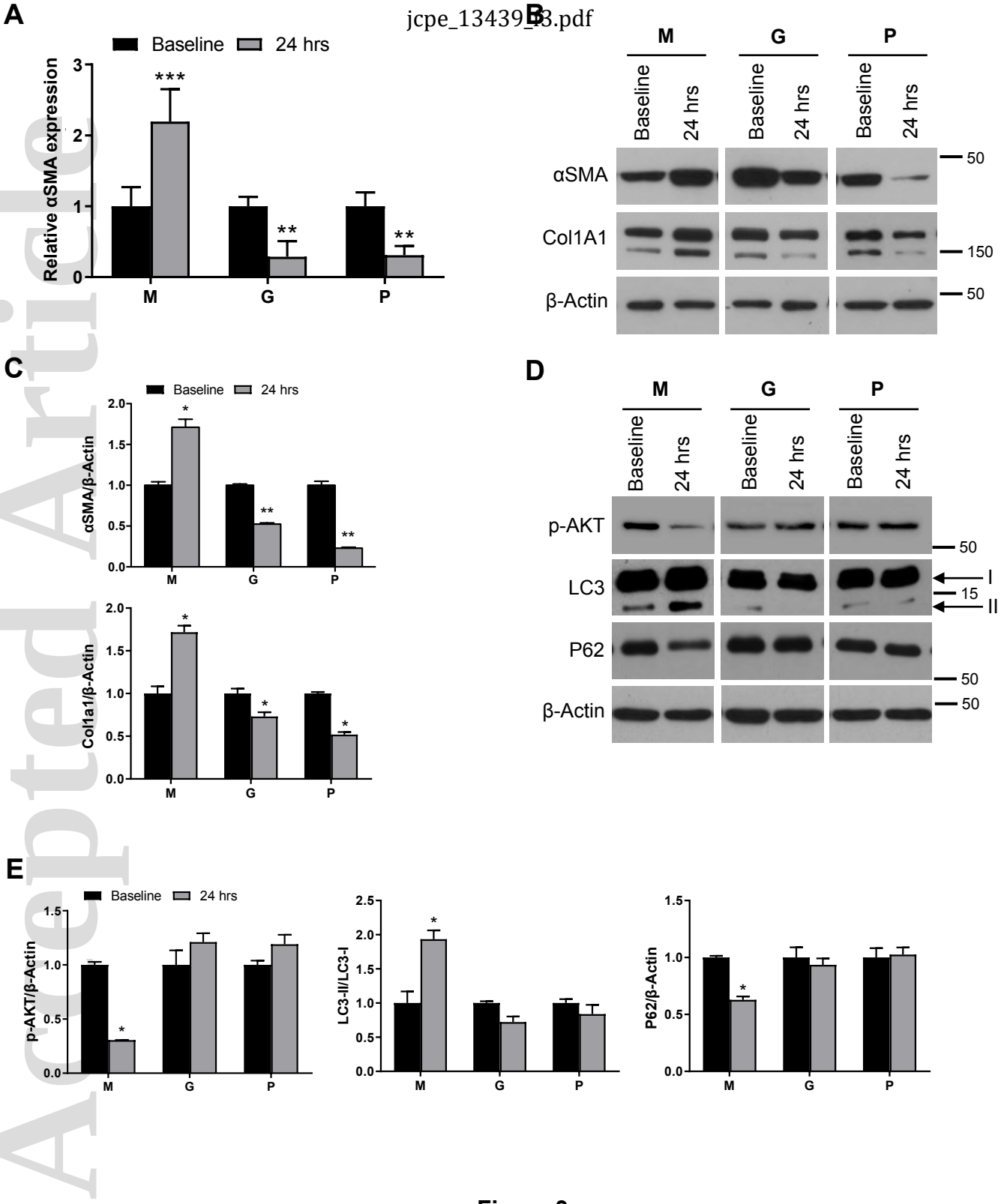

Figure 3

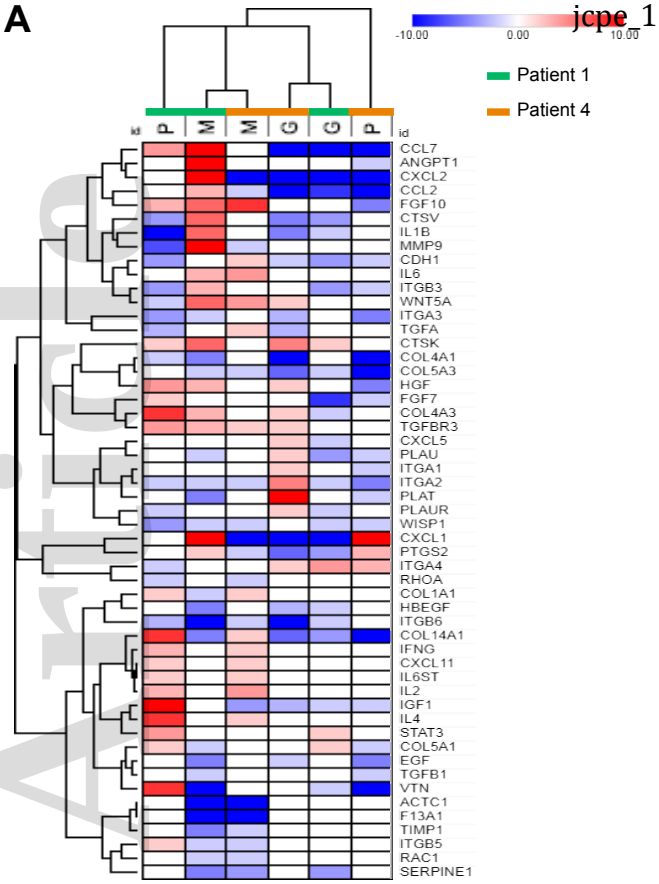

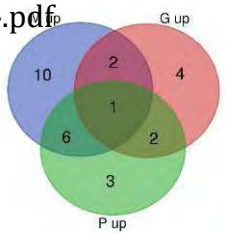

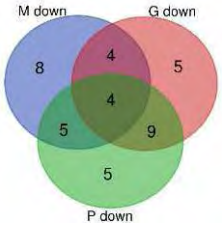

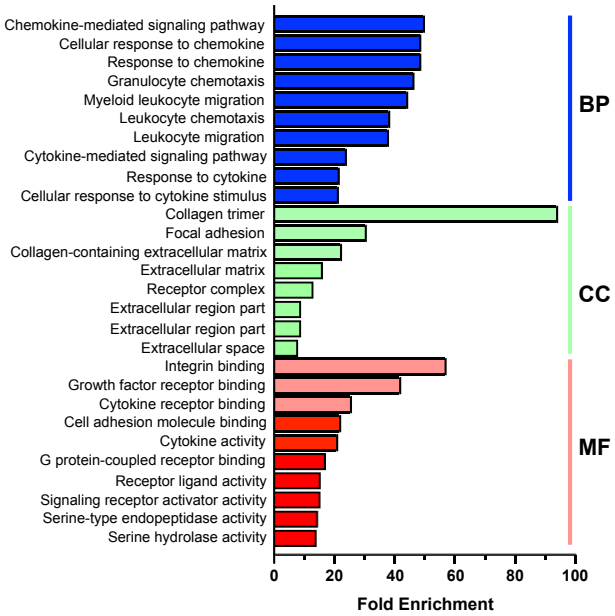

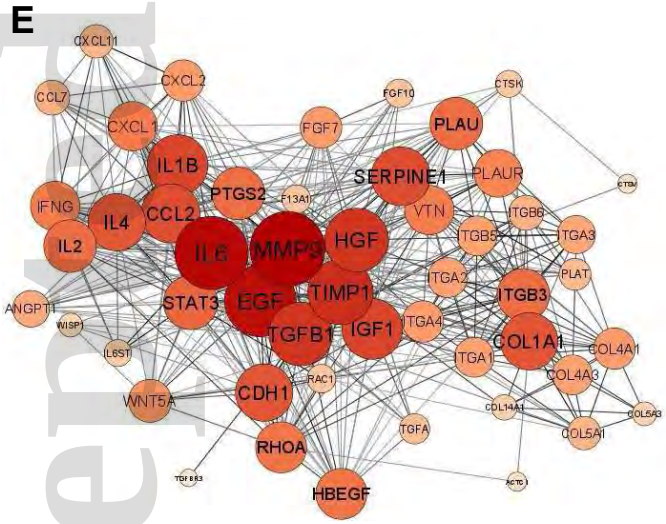

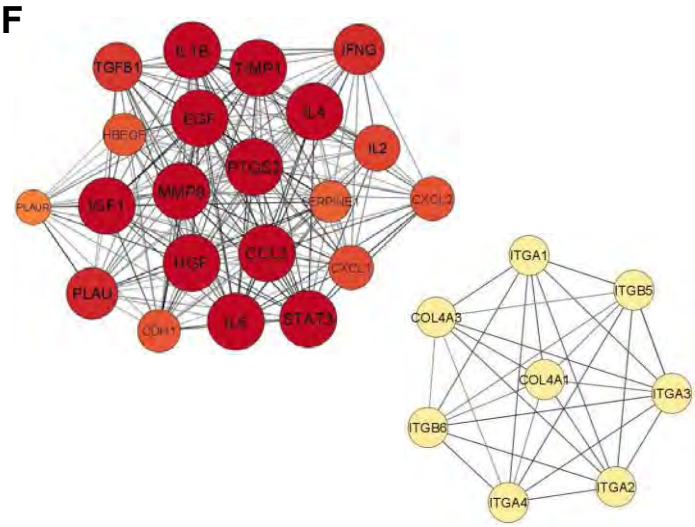

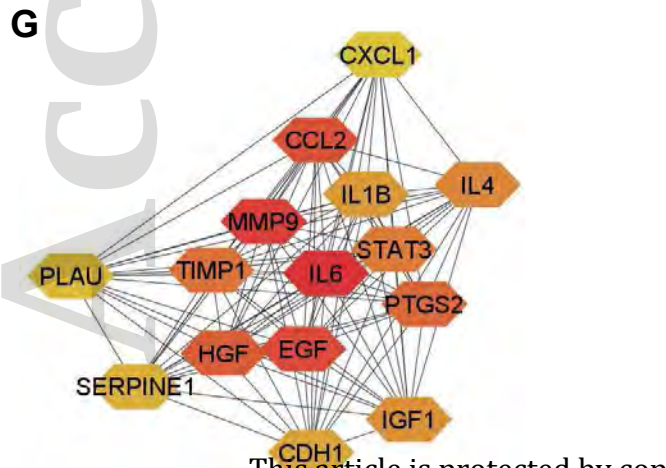

H

Gene symbol	Modulation					
	M		G		P	
	P1	P4	P1	P4	P1	P4
RAC1	↓	↓	-	-	-	-
SERPINE1	↓	↓	-	↓	-	-
TIMP1	↓	↓	-	-	-	-
CDH1	-	↑	↓	↓	↓	↓
ITGA4	-	-	↑	↑	↓	↑
ITGB5	↓	↓	-	-	↑	-
IL6	↑	↑	-	-	-	-
CXCL1	↑	↓	↓	↓	-	↑

Figure 4

A

Gene symbol	Modulation		
	M	G	P
RAC1	↓	↑	-
SERPINE1	↑	-	↓
TIMP1	↑	-	↓
CDH1	-	↓	↓
ITGA4	↓	↑	↑
ITGB5	-	-	↓
IL6	-	↓	↓
CXCL1	↑	↓	↑

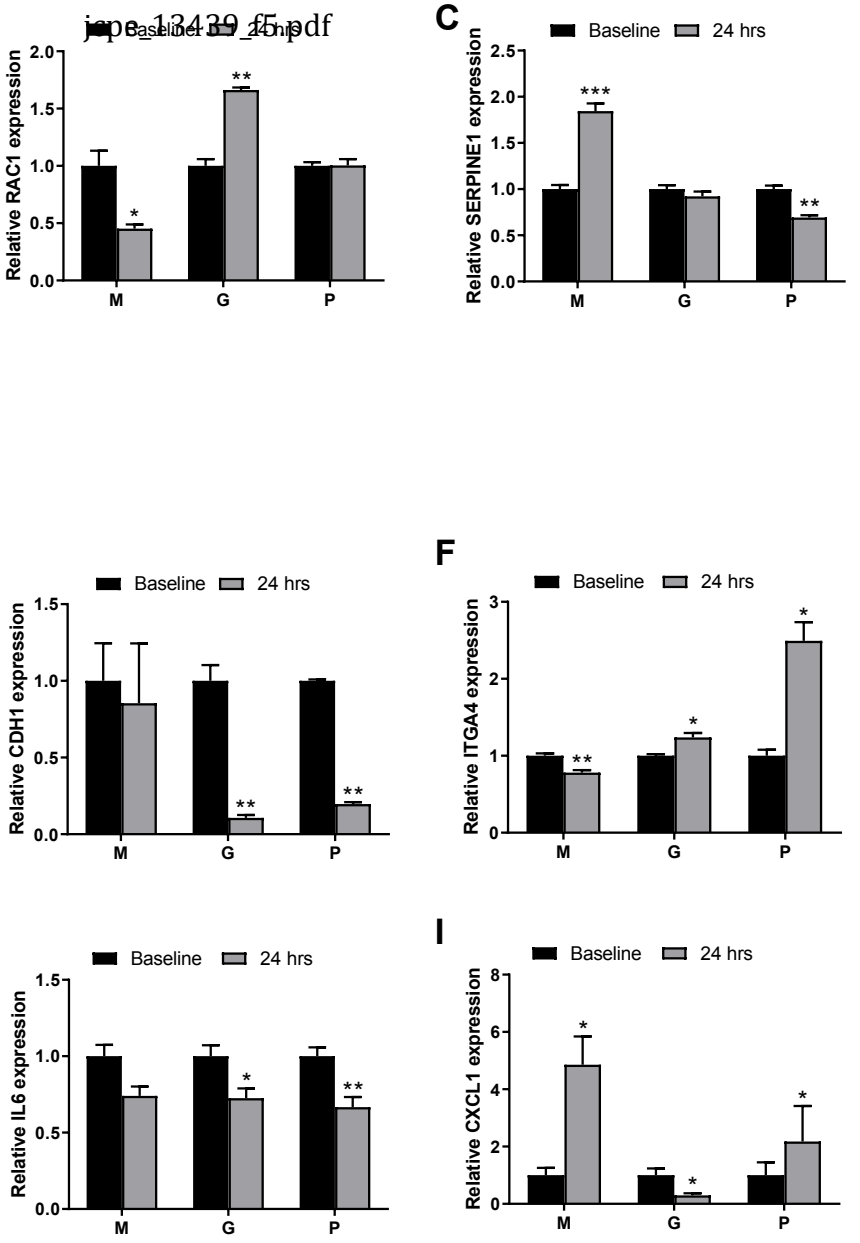

Figure 5

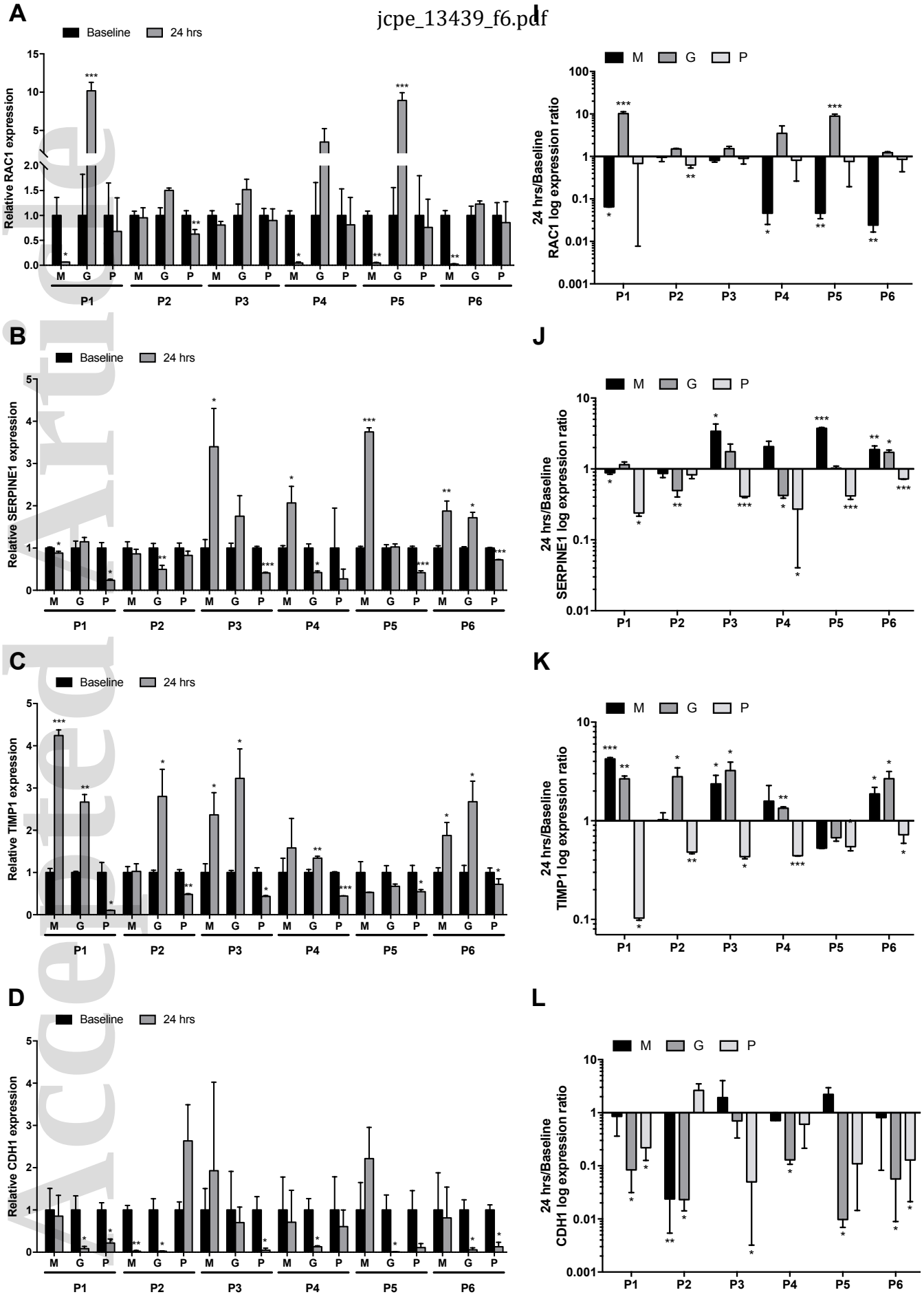

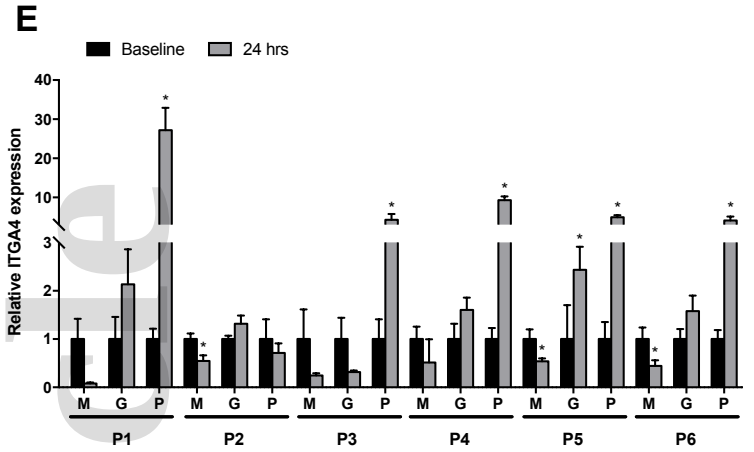

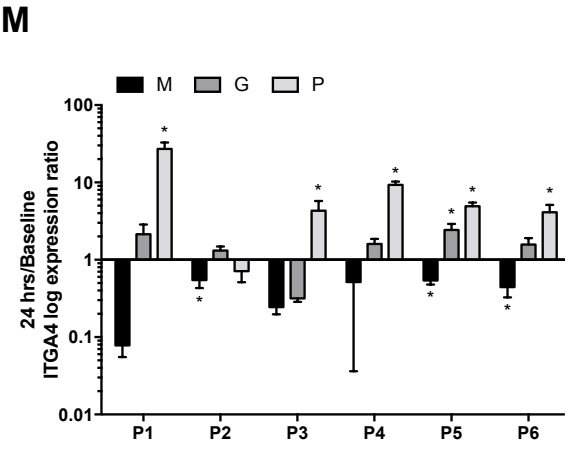

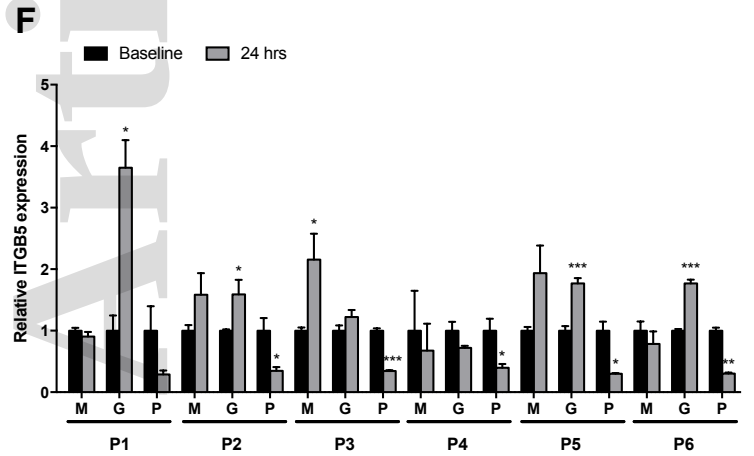

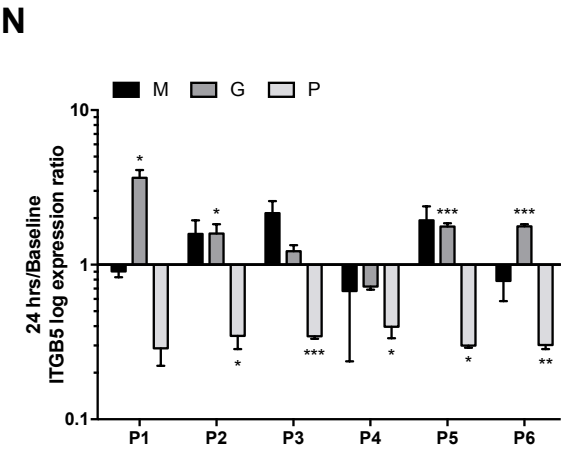

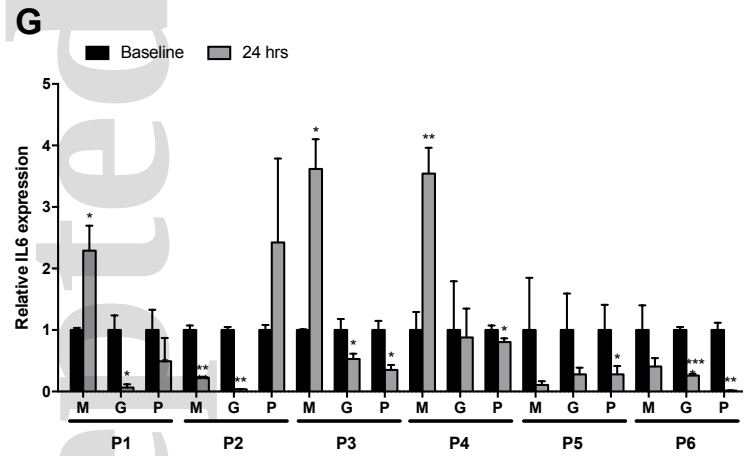

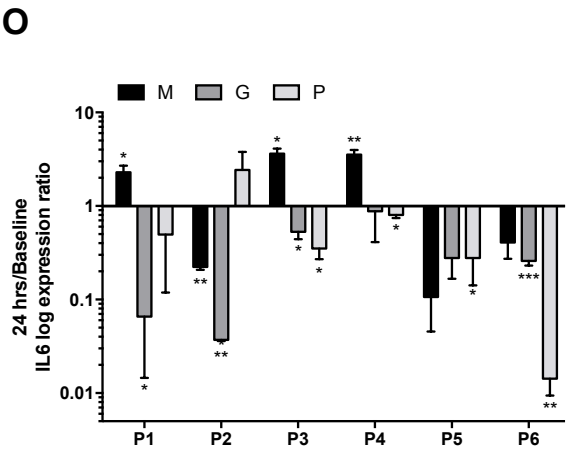

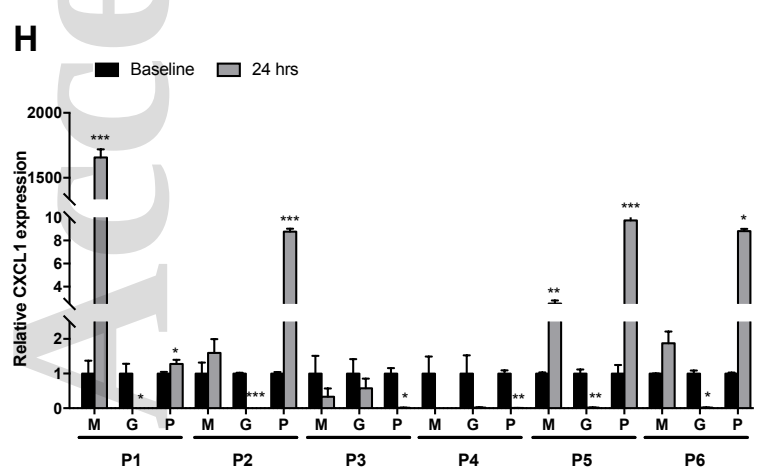

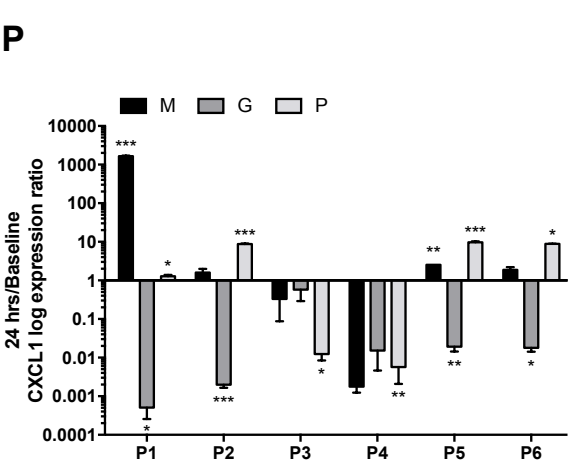

Figure 6